Charge accumulation in GaAs/AlGaAs triple barrier resonant tunneling structures

P. D. Buckle, P. Dawson, C. Y. Kuo, A. H. Roberts, W. S. Truscott, M. Lynch, and M. Missous

Citation: Journal of Applied Physics **83**, 882 (1998); doi: 10.1063/1.366772
View online: http://dx.doi.org/10.1063/1.366772
View Table of Contents: http://scitation.aip.org/content/aip/journal/jap/83/2?ver=pdfcov
Published by the AIP Publishing

Charge accumulation in GaAs/AlGaAs triple barrier resonant tunneling structures

P. D. Buckle[a] and P. Dawson[b]
Department of Physics, University of Manchester Institute of Science and Technology, PO Box 88, Manchester, M60 1QD, United Kingdom

C. Y. Kuo, A. H. Roberts, W. S. Truscott, M. Lynch, and M. Missous
Department of Electrical Engineering and Electronics, University of Manchester Institute of Science and Technology, PO Box 88, Manchester M60 1QD, United Kingdom

(Received 3 June 1997; accepted for publication 7 October 1997)

In this article we present photoluminescence and photoluminescence excitation spectroscopy data from three triple barrier resonant tunneling structures. The spectroscopic techniques are used to estimate the charge accumulation in both tunneling quantum wells of the devices as a function of bias. The charging behavior is extremely asymmetrical, with significant charge accumulation only in the quantum well adjacent to the emitter region of the device and not in the quantum well adjacent to the collector region, irrespective of the direction of bias. This asymmetry in the charging behavior is analogous to highly asymmetrical double barrier resonant tunneling structures. However, due to the two quantum wells present in the triple barrier design it provides a more flexible system to study charge density dependent effects. We also present evidence for negatively charged exciton formation in the first quantum well for both directions of applied bias. © *1998 American Institute of Physics.* [S0021-8979(98)04502-2]

INTRODUCTION

Ever since the pioneering work of Esaki and Tsu semiconductor resonant tunneling structures have been the subject of a great deal of interest, not only from the purely scientific view but also for incorporation in commercial device structures.[1–3] The main interest has been in double barrier resonant tunneling structures (DBRTSs) where most of the effort has been centered around the possibility of exploiting such structures for high speed device operation,[4,5] either as oscillators and mixers, or as fast switches. A phenomenon that can influence not only device operation but is also of interest in its own right is that of charge accumulation in both the emitter and the quantum well. The understanding of this charging behavior is important for the accurate calculation of electric field distributions across the structure and has been used to explain the observation of intrinsic device bistability observed in the current versus voltage $[I(V)]$ characteristic.[6–8]

Optical spectroscopy has proven to be a very fruitful technique for monitoring the charging behavior of DBRTS. The first observation of photoluminescence (PL) from the quantum well of a DBRTS was by Young *et al.*[9] Holes, photocreated in the top contact region of the device are swept into the quantum well by the applied field where they recombine with electrons injected from an *n* doped bottom contact. It was shown by Skolnick *et al.*[10] that band filling effects on the PL line width can provide a direct measure of charge build up in the quantum well of DBRTS as a function of bias. While Fisher *et al.*[11] demonstrated that PL measurements could be used successfully to probe the charge accumulation in the two-dimensional (2D) emitter region of a modified GaAs/AlGaAs DBRTS which incorporated an InGaAs prewell layer to inhibit the movement of holes away from the emitter region.

TBRTSs have, in general, received less attention than DBRTS. From the device standpoint TBRTS have proved, until now, to have limited advantages over conventional DBRTS. However interest in these systems, where quantum well confined states can be resonantly coupled by the application of an applied bias, is increasing. A large amount of this interest is generated by the possibility of altering electron populations in the quantum wells of the device, creating the conditions for intersubband lasing, by manipulating intersubband scattering rates.[12] Interest has also been generated by the possibility of creating multistate logic and memory devices by exploiting $I(V)$ characteristics that have multiple negative differential resistance (NDR) regions where the peak resonant currents are of similar magnitude.[13]

Continuous wave PL measurements have been used to investigate the subband structure of TBRTS devices, two examples of which are the observation of cross barrier recombination in both unipolar *n*-type TBRTS,[14] and bipolar TBRTS.[15] Furthermore, time resolved PL spectroscopy has been used to determine carrier transport times through TBRTS.[16]

In this article we present low temperature PL and PL excitation (PLE) measurements on a series of GaAs/AlGaAs TBRTS with symmetric and asymmetric quantum wells. From these measurements we have demonstrated that charge accumulation occurs only in the quantum well adjacent to the bulk emitter layer, and not in the quantum well adjacent to the collector, irrespective of the direction of applied bias. This observation is in good agreement with the charge accumulation calculated using a self-consistent theoretical model.

[a]Also at the Department of Electrical Engineering and Electronics, University of Manchester Institute of Science and Technology, PO Box 88, Manchester M60 1QD, United Kingdom.
[b]Corresponding author; electronic mail: philip.dawson@umist.ac.uk

 0021-8979/98/83(2)/882/6/$15.00

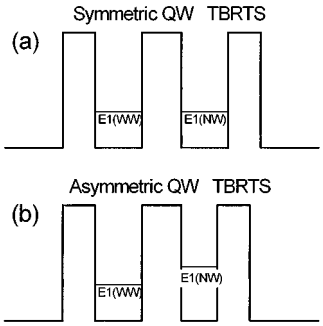

FIG. 1. Schematic band alignments for asymmetric and symmetric quantum well TBRTS's.

This charging behavior results in a system more clearly suited for the observation of the effects of charge accumulation in the quantum wells, and we go on to present evidence for negatively charged exciton (X^-) formation in the emitter quantum well of the TBRTS. This is shown to be unambiguously associated with charge build up due to the asymmetric charging behavior of these devices.

EXPERIMENTAL DETAILS

The measurements were carried out on a series of GaAs/$Al_{0.30}Ga_{0.70}As$ TBRTS structures grown by molecular beam epitaxy (MBE) in a VG Semicon V90H system at a growth temperature of 580 °C using conventional Ga and Al cells and a solid source cracker producing As_2. The structures were grown on semi-insulating GaAs substrates with a layer sequence as follows: (i) 1 μm thick Si doped ($n=7\times10^{18}$ cm^{-3}) GaAs buffer layer; (ii) 100 Å thick Si doped ($n=3\times10^{18}$ cm^{-3}) GaAs layer; (iii) 200 Å thick undoped GaAs spacer layer; (iv) 45 Å thick $Al_{0.3}Ga_{0.7}As$ barrier layer; (v) 67 Å nominally undoped GaAs quantum well; (vi) 54 Å thick $Al_{0.3}Ga_{0.7}As$ barrier layer; (vii) GaAs quantum well of widths 56 and 48 Å (samples A and B, respectively—asymmetric quantum well devices), and 67 Å (sample C—symmetric quantum well device); (viii) 45 Å $Al_{0.28}Ga_{0.72}As$ barrier layer; (ix) 200 Å undoped GaAs layer; and (x) 0.5 μm thick Si doped ($n=7\times10^{18}$ cm^{-3}) GaAs contact layer. This is subsequently referred to as the ''top contact.''

Schematic diagrams showing the conduction band edge profiles and the lowest confined electron states for both symmetric and asymmetric structures are shown in Fig. 1. Devices were processed by conventional photolithography into a double step mesa with a 80 μm×80 μm active region (top mesa). Ohmic contacts were formed on the top and bottom mesas by evaporating AuGe/Ni/Au and alloying at 450 °C for 30 s by rapid thermal annealing. Devices were mounted on 20-way ceramic packages, and clamped to the cold finger of a variable temperature (6–300 K) closed cycle helium cryostat. $I(V)$ characteristics were measured using a four terminal technique with a HP4142B source/measurement system. PL and PLE measurements were performed by exciting through the top contact using light from a chopped tunable Ti:sapphire laser as the excitation source, and the resultant luminescence was dispersed with a 0.75 m double grating spectrometer (Spex 1404) and detected by a thermo-

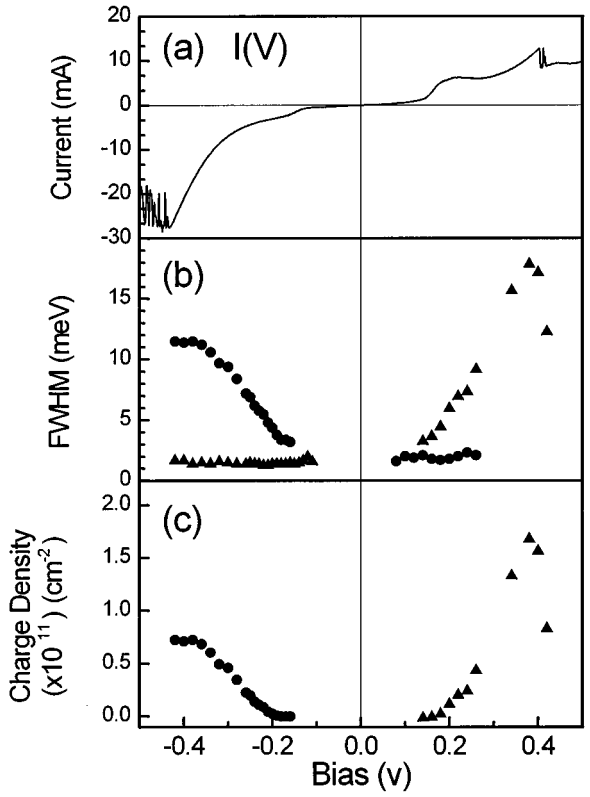

FIG. 2. (a) $I(V)$ characteristic for sample A (asymmetric quantum well TBRTS. (b) FWHM for the E1–HH1(WW) and E1–HH1(NW) PL transitions for both forward and reverse bias conditions. (c) Charge density in the wide (▲) and narrow (●) quantum wells, deduced from the PL lineshape, as a function of forward and reverse bias.

electrically cooled GaAs photomultiplier followed by a lock-in detector. The incident laser power density ($\sim$100 mW/cm^2) was kept at a level which did not significantly perturb the $I(V)$ characteristics of the illuminated devices.

RESULTS

The $[I(V)]$ characteristic for sample A recorded at 6 K is shown in Fig. 2(a). For the purposes of this discussion we define forward bias as that which corresponds to the top contact being positive. It is important to emphasize that under forward bias the wide quantum well is adjacent to the emitter layer, whereas in reverse bias the narrow quantum well is adjacent to the emitter. The quantum well adjacent to the emitter layer is defined as the emitter quantum well and the other quantum well in the structure defined as the collector quantum well. In either bias direction the main resonances (0.4 V forward bias, 0.42 V reverse bias) are attributed to the $n=1$ electron state in the emitter quantum well aligning with a quasiconfined state in the emitter region, formed by band bending due to charge accumulation at the emitter barrier. The emitter quantum well $n=1$ state remains on resonance over a relatively large bias range because of charge accumulation in the quantum well, in a similar manner to the behavior of a highly asymmetric DBRTS.[17] The $n=1$ state in the emitter quantum well remains pinned to the emitter state due

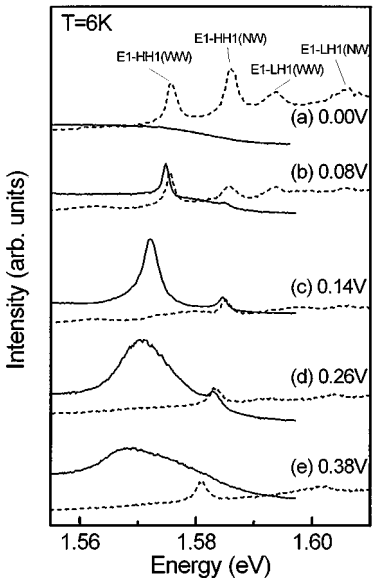

FIG. 3. PL (solid lines) and PLE (broken lines) for zero bias and a range of forward biases up to the peak of the resonant current for sample A.

to an electrostatic feedback process, whereby pinning is sustained because small changes in the applied voltage are electrostatically compensated by a change in the charge accumulation in the quantum well.[18] This charge build up is demonstrated in the optical measurements described later. The feature at 0.42 V is attributed to LO phonon assisted tunneling processes.[18,19] In either bias direction the first quantum well state to fall below the Fermi energy of the emitter is the $n=1$ electron state in the collector quantum well. However, if the emitter quantum well is wide it can fall below the Fermi energy in the emitter before the collector state effectively goes off resonance. The features observed at 0.2 and 0.18 V in the forward and reverse bias directions, respectively, are attributed to the superposition of the effects of the collector quantum well resonantly aligning with the emitter state and the onset of tunneling through the $n=1$ emitter quantum well as it falls below the emitter Fermi energy.

The results of PL (solid lines) and PLE (broken lines) experiments on sample A (asymmetric quantum well TBRTS) as a function of forward bias are shown in Fig. 3. The wide quantum well (WW) is adjacent to the emitter in the forward bias direction (emitter quantum well) and so is the first tunneling well of the TBRTS. Figure 3(a) shows PL and PLE spectra at zero applied bias. No luminescence is observed from the quantum well region due to the fast escape of directly photoexcited electrons through the confining barriers. However, in the PLE experiment, by monitoring the luminescence from the heavily doped contact region we can observe transitions in both quantum wells associated with the $n=1$ electron ($E1$) and $n=1$ heavy and light hole ($HH1$ and $LH1$, respectively) subbands. The process by which these transitions are observed is described in more detail elsewhere.[20] The peaks in the PLE spectra are assigned, as indicated in Fig. 3(a), to exciton creation involving $E1$ and $HH1$ and $LH1$ states in the NW and WW. The assignment of the transitions involved is made by comparison with the results from a square well calculation using effective masses of $m_c^*=0.067$, $m_{HH}^*=0.34$, and $m_{LH}^*=0.095$ for the electron, heavy hole, and light holes, respectively, a conduction:valence band offset ratio of 66:34, the nominal quantum well thicknesses and barrier compositions and the appropriate exciton binding energies.[21]

Figure 3(b) shows 6 K PL and PLE spectra close to the onset of resonance (0.08 V) in the forward bias direction over the energy region where we might expect to observe PL from the quantum wells. There are two peaks observed in the PL spectrum at energies of 1.575 and 1.585 eV. The peaks are attributed to excitonic recombination involving $E1$ electrons and $HH1$ holes in the WW and NW of the TBRTS (labeled $E1-HH1$(WW) and $E1-HH1$(NW), respectively). The broad background of luminescence beneath these peaks originates from the heavily doped top contact layer of the device ($n=7\times10^{18}$ cm^{-3}). The assignment of the quantum well recombination processes is based on the comparison with the PLE spectrum [Fig. 3(b)]. Note that due to the detection mechanism employed for the PLE measurement the spectrum extends to energies below the $E1-HH1$(WW) PL peak.

Figures 3(c)–3(e) show the evolution of the PL and PLE spectra as a function of forward bias up to the maximum resonant device current (0.38 V≡on resonance). The $E1-HH1$(WW) PL peak broadens with increasing bias until at 0.38 V the FWHM is 18 meV. As the $E1-HH1$(WW) PL recombination broadens the $E1-HH1$(WW) and $E1-LH1$(WW) PLE peaks weaken rapidly and by 0.14 V [Fig. 3(c)] are no longer clearly resolved. The quenching of the $E1-HH1$(WW) and $E1-LH1$(WW) PLE peaks, and the broadening of the $E1-HH1$(WW) PL peak are both indicative of the existence of a large carrier density in the WW. The behavior of the $E1-HH1$(WW) PL peak is in contrast to the $E1-HH1$(NW) PL peak which has a constant line width (FWHM $\sim$1.8 meV) over the same forward bias range, also the $E1-HH1$(NW) and $E1-LH1$(NW) PLE peaks remain strong. This enables us to measure a Stokes shift between the $E1-HH1$(NW) PL peak and $E1-HH1$(NW) PLE peak which remains constant ($\sim$0.4 meV) up to high bias. The movement to lower energy of the NW PL peak and PLE peaks with increasing bias is attributed to the quantum confined Stark effect.[22]

The line shape broadening of the WW PL peak and quenching of the WW PLE transitions is in contrast to that observed in the reverse bias direction where the narrow well becomes the quantum well adjacent to the emitter. PL (solid lines) and PLE (broken lines) spectra from the same device in reverse bias are shown in Fig. 4. The PLE measurements are recorded using the same detection technique where luminescence from the heavily doped contact region is monitored. The onset of the luminescence in reverse bias occurs at -0.09 V. Figures 4(a)–4(b) show the evolution of the PL spectra with increasing reverse bias. In contrast to the forward bias direction the $E1-HH1$(NW) PL peak broadens significantly (FWHM changes from 2 to 11.5 meV), there is also a corresponding quenching of the $E1-HH1$(NW) PLE transitions [Fig. 4(b)–4(d)]. The $E1-HH1$(WW) PL line

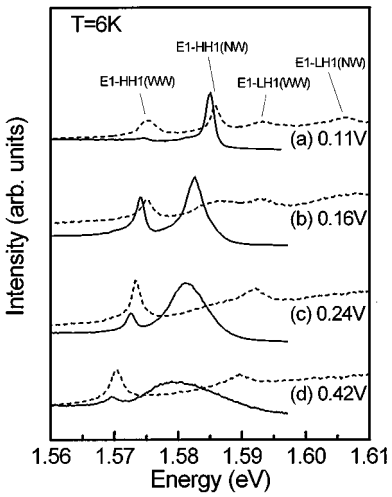

FIG. 4. PL (solid lines) and PLE (broken lines) for a range of reverse biases up to the peak of resonant current for sample A.

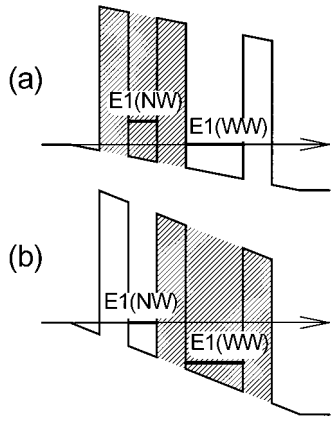

FIG. 5. Schematic conduction band diagram of an asymmetric TBRTS, (a) under bias conditions where electrons in the emitter are able to tunnel through the WW (collector quantum well); (b) under bias conditions where electrons in the emitter region are able to tunnel through the NW.

width remains unchanged in reverse bias with a small associated Stokes shift between the $E1-HH1$(WW) PL and PLE transitions. The $E1-HH1$(WW) and $E1-LH1$(WW) PLE transitions remain well resolved up to a bias of 0.42 V. The measured line widths of the $E1-HH1$(WW) and $E1-HH1$(NW) PL peaks are plotted as a function of both reverse and forward bias in Fig. 2(b).

DISCUSSION

The PL line width increase, coupled with the quenching of the excitonic transition in the PLE spectra associated with the same quantum well is evidence for charge accumulation. At carrier concentrations where the exciton transition is no longer observable in the PLE spectrum the recombination is assumed to be predominantly free carrier in nature involving electron states at wave vector $k=0$ up to states corresponding to the Fermi energy E_{f}, with photocreated localized holes.[23] The width of the PL spectrum is determined by E_f, with a fall off in intensity towards E_f which depends on the degree of hole localization or disorder in the system.[24,25] The broadening of the PL peak is therefore associated with charge accumulation in the quantum well region. We therefore conclude from Fig. 1(b) that significant charge accumulation occurs in the quantum well adjacent to the emitter irrespective of well width, and not in the second quantum well. Due to the quenching of the exciton transitions in the PLE spectra at high biases it is not possible to use the energy difference between the energy of the luminescence peak, and the exciton peak in the PLE spectra to determine the extent of the charge accumulation in the emitter quantum well. However, as an estimate of the magnitude of charge density we have employed a line shape analysis that has been shown previously to be successful in quantifying charge build up.[10] Charge densities were estimated from values of E_f, deduced from a line shape analysis of the PL spectra. This was achieved by comparison with a convolution of the lowest bias PL line shape observable and a Fermi function together with an exponential fall off factor representing the decreasing oscillator strength for nonwavevector conserving transitions.

We have plotted estimated charge densities using this technique as a function of bias in Fig. 2(c). The maximum charge density in the NW in reverse bias is $\sim 0.8 \times 10^{11}$ cm^{-2}, whereas the maximum charge density in the WW in forward bias is $\sim 1.2 \times 10^{11}$ cm^{-2}. The charge density drops rapidly in either bias direction as the device goes off resonance, i.e., the respective $n=1$ electron state of the emitter quantum well falls below the confined state in the emitter region.

This charging behavior can be understood by analogy with a highly asymmetric double barrier structure.[17] A schematic conduction band potential profile of an asymmetric TBRTS is shown in Fig. 5 for different values of applied reverse bias. At low reverse bias (narrow well adjacent to the emitter) the wide well $n=1$ electron state is the first to align with the emitter states. However the probability of coherent tunneling from the emitter directly into the wide well is small. The NW region together with the confining barriers can be considered to act as a thick potential barrier [shown as a shaded region in Fig. 5(a)]. This is therefore analogous to an asymmetric DBRTS where the emitter barrier is very thick and the collector barrier is thin. Any electrons that do tunnel through to the WW can easily tunnel through the collector barrier, and so there is no significant charge accumulation in the wide well at this bias [Fig. 4(b)]. As the reverse bias is increased the $n=1$ electron state in the narrow well aligns with the emitter state. Electron tunneling can now occur from the emitter to the NW. However the carrier escape from the narrow well is now inhibited by the WW region which is no longer on resonance with the NW $n=1$ electron state, or the emitter state. The wide well region now acts like a wide potential barrier to the narrow well confined electrons: the total device behaving like an asymmetrical DBRTS where the emitter barrier is thin and the collector barrier is thick. Thus significant charge accumulates in the NW [Fig. 4(c)]. In the forward bias direction the situation is very similar. As the bias is increased the $n=1$ NW electron

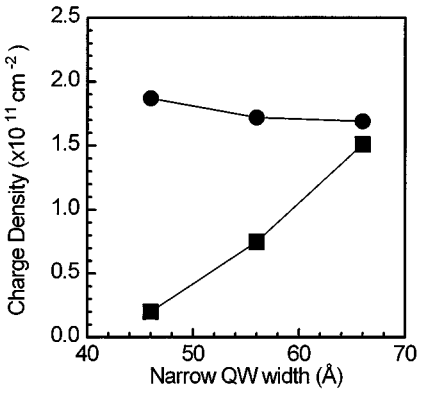

FIG. 6. Charge densities in the wide (●) and narrow (■) quantum wells of the three TBRTS at the peak of forward and reverse bias resonant current, respectively.

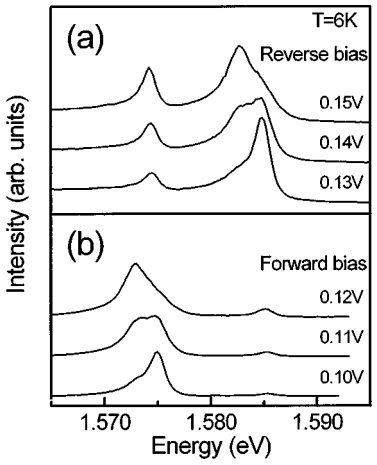

FIG. 7. PL spectra at the onset of significant device current in (a) forward bias and (b) reverse bias.

state will align with the emitter states, and the device will again resemble an asymmetric DBRTS with a thick emitter barrier and a thin collector barrier. On a further increase in bias the WW $n=1$ electron state aligns with emitter states. The device resembles an asymmetric DBRTS with a thick collector barrier, and so charge builds up in the WW. The only difference between reverse and forward bias directions is the voltage which must be applied to achieve tunneling into the emitter quantum well. In reverse bias the emitter well is narrow, and so a larger voltage must be applied to align the confined electron state with the emitter electrons than with the wide well in forward bias. Therefore, due to the increased field across the active region the effective collector barrier will be greater in reverse bias and should accumulate more charge (with a correspondingly higher voltage at peak resonant current). This is supported both by the charge densities estimated from the line shape analysis [Fig. 2(c)], and from the asymmetry in the $I(V)$ characteristic [Fig. 2(a)].

This analogy with asymmetrical DBRTS is applicable to all TBRTS where alignment of the two quantum well confined states in forward bias does not coincide with alignment of the states with the emitter. To demonstrate this we have performed the same spectroscopic measurements on TBRTS with increased asymmetry between the quantum well thicknesses (sample B) and nominally symmetric quantum wells (sample C). The charge density deduced from line shape analysis for each structure is plotted as a function of NW width in Fig. 6. The charge accumulation in the WW in forward bias remains essentially the same for all three samples (A, B, and C), whereas the NW charge accumulation decreases as the width of the narrow well is reduced. This is consistent with the asymmetric DBRTS analogy.

Since charge accumulates in the different wells in the forward and reverse bias directions we can clearly distinguish charge density dependent behavior from other tunneling phenomena such as localized impurity tunneling.[26] Figure 7(a) shows a series of PL spectra from sample A over a very small range of reverse bias. There are clearly two features associated with recombination in the NW. The luminescence peak at ~ 1.585 meV remains at a constant energy over the small bias range displayed. However at 0.13 V a second feature emerges at an energy of ~ 1.583 meV, and as the bias is increased emerges as the dominant feature in the spectrum. By 0.15 V the original peak at 1.585 meV has been effectively suppressed. This bias range corresponds to the onset of significant charge accumulation in the well [see Fig. 2(c)]. However there is no evidence for any splitting of the $E1-HH1$(WW) luminescence spectrum at any value of reverse bias. Figure 7(b) shows a similar series of PL spectra from sample A over a small forward bias range. Two peaks are now observed in the $E1-HH1$(WW) PL peak (0.11 V) with no corresponding feature in the $E1-HH1$(NW) spectrum. This is effectively the opposite behavior to the reverse bias direction where the double peak is observed in the $E1-HH1$(NW) luminescence. The additional PL line is not observed in the collector quantum well luminescence in either bias direction which strongly suggests that this is a phenomenon associated with the charge accumulation within the emitter quantum well. We suggest that as the energy splitting between the two features is ~ 2 meV and that the appearance of the low energy feature is associated with significant charge accumulation that this feature is due to recombination of negatively charged excitons (X^-) as reported in double barrier devices by Buhman *et al.*[27]

The splitting observed in the luminescence spectra shown in Fig. 7 cannot be accounted for by quantum well state coupling. The calculated results of a fully self-consistent coherent tunneling model including both the triple barrier structure and the heavily doped emitter region show that the symmetric/antisymmetric splitting, when the $n=1$ states cross in the forward bias direction is ~ 1.3 meV. Also, more importantly, due to the asymmetric nature of the triple barrier structure, the $n=1$ electron states never cross in the reverse bias direction and as the experimentally observed splitting is seen in both bias directions the observed splitting cannot be accounted for by quantum well state coupling.

SUMMARY

In conclusion, we have studied the charge accumulation in a series of triple barrier resonant tunneling structures. In

these structures charge build up is observed in the emitter quantum well only, irrespective of the direction of bias, while the collector quantum well remains uncharged in either bias direction. This charging behavior is similar in manner to that observed in asymmetric double barrier structures where the thick collector barrier inhibits carriers escaping the quantum well region. Under the conditions where there is significant charge build up in the individual quantum wells, we can clearly observe features in the PL spectra due to the recombination of negatively charged excitons.

ACKNOWLEDGMENTS

The work described in this article was carried out with the financial support of the United Kingdom Engineering and Physical Sciences Research Council.

[1] L. Esaki and R. Tsu, IBM J. Res. Dev. **14**, 61 (1970).
[2] R. Tsu and L. Esaki, Appl. Phys. Lett. **22**, 562 (1973).
[3] L. L. Chang, L. Esaki, and R. Tsu, Appl. Phys. Lett. **24**, 593 (1974).
[4] T. C. L. G. Sollner, H. Q. Lee, A. Correa, and W. D. Goodhue, Appl. Phys. Lett. **47**, 1319 (1984).
[5] T. C. L. G. Sollner, E. R. Brown, W. D. Goodhue, and H. Q. Lee, Appl. Phys. Lett. **50**, 332 (1987).
[6] V. J. Goldman, D. C. Tsui, and J. E. Cunningham, Phys. Rev. Lett. **58**, 1256 (1987).
[7] A. Zaslavsky, V. J. Goldman, D. C. Tsui, and J. E. Cunningham, Appl. Phys. Lett. **50**, 1281 (1988).
[8] E. S. Alves, L. Eaves, M. Henini, O. H. Hughes, M. L. Leadbeater, F. W. Sheard, and G. A. Toombs, Electron. Lett. **24**, 1190 (1988).
[9] J. F. Young, B. M. Wood, G. C. Aers, R. L. Devine, M. C. Lui, D. Landheer, M. Buchanan, A. J. Springthorpe, and P. Mandeville, Phys. Rev. Lett. **60**, 2085 (1988).
[10] M. S. Skolnick, D. G. Hayes, P. E. Simmonds, A. W. Higgs, G. W. Smith, H. J. Hutchinson, C. R. Whitehouse, L. Eaves, M. Henini, O. H. Hughes, M. L. Leadbeater, and D. P. Halliday, Phys. Rev. B **41**, 10 754 (1990).
[11] T. A. Fisher, P. D. Buckle, P. E. Simmonds, R. J. Teissier, M. S. Skolnick, C. R. H. White, D. M. Whittaker, L. Eaves, B. Usher, P. C. Kemeny, R. Grey, G. Hill, and M. A. Pate, Phys. Rev. B **50**, 18 469 (1994).
[12] A. Kastalsky, V. J. Goldman, and J. H. Abeles, Appl. Phys. Lett. **59**, 2636 (1991).
[13] H. Mizuta, T. Tanoue, and S. Takahashi, IEEE Trans. Electron Devices **35**, 1951 (1988).
[14] T. S. Turner, P. M. Martin, L. Eaves, H. B. Evans, P. A. Harrison, M. Henini, O. H. Hughes, D. M. Whittaker, P. D. Buckle, T. A. Fisher, M. S. Skolnick, and G. Hill, Solid-State Electron. **37**, 721 (1994).
[15] P. A. Harrison, L. Eaves, P. M. Martin, M. Henini, P. D. Buckle, M. S. Skolnick, D. M. Whittaker, and G. Hill, Surf. Sci. **305**, 353 (1994).
[16] D. Bertram, H. T. Grahn, C. Van Hoof, J. Genoe, G. Borghs, W. W. Ruhle, and K. von Klitzing. Phys. Rev. B **50**, 17 309 (1994).
[17] L. Eaves, G. A. Toombs, F. W. Sheard, C. A. Payling, M. L. Leadbeater, E. S. Alves, T. J. Foster, P. E. Simmonds, M. Henini, O. H. Hughes, J. C. Portal, G. Hill, and M. A. Pate, Appl. Phys. Lett. **52**, 212 (1988).
[18] V. J. Goldman, D. C. Tsui, and J. E. Cunningham, Phys. Rev. B **36**, 7635 (1987).
[19] M. L. Leadbeater, O. H. Hughes, E. S. Alves, L. Eaves, M. Henini, G. A. Toombs, and F. W. Sheard, J. Phys.: Condens. Matter **1**, 10 605 (1989).
[20] P. D. Buckle, P. Dawson, M. Missous, and W. S. Truscott, J. Cryst. Growth **175/176**, 1299 (1997).
[21] P. Dawson, K. J. Moore, G. Duggan, H. I. Ralph, and C. T. B. Foxon, Phys. Rev. B **34**, 6007 (1986).
[22] D. A. B. Miller, D. S. Chemla, T. C. Damen, A. C. Gossard, W. Wiegmann, T. H. Wood, and C. A. Burrus, Phys. Rev. B **32**, 1043 (1985).
[23] M. S. Skolnick, K. J. Nash, M. K. Saker, S. J. Bass, P. A. Claxton, and J. S. Roberts, Appl. Phys. Lett. **50**, 1885 (1987).
[24] M. S. Skolnick, J. M. Rorison, K. J. Nash, D. J. Mowbray, P. R. Tapster, S. J. Bass, and A. D. Pitt, Phys. Rev. Lett. **58**, 2130 (1987).
[25] S. K. Lyo and E. D. Jones, Phys. Rev. B **38**, 4113 (1988).
[26] M. W. Dellow, P. H. Beton, C. J. G. M. Langervak, T. J. Foster, P. C. Main, L. Eaves, M. Hennini, S. P. Beaumont, and C. D. W. Wilkinson, Phys. Rev. Lett. **68**, 1754 (1992).
[27] H. Buhmman, L. Mansouri, J. Wang, P. H. Beton, N. Mori, L. Eaves, M. Henini, and M. Potemski, Phys. Rev. B **51**, 7969 (1995).